Pharmaceutical Research, Vol. 23, No. 12, December 2006 (© 2006)
DOI: 10.1007/s11095-006-9090-6

Research Paper

Fractal Michaelis-Menten Kinetics Under Steady State Conditions: Application to Mibefradil

Rebeccah E. Marsh[1,2] and Jack A. Tuszyński[1]

Received March 18, 2006; accepted June 9, 2006; published online October 25, 2006

Purpose. To provide the first application of fractal kinetics under steady state conditions to pharmacokinetics as a model for the enzymatic elimination of a drug from the body.
Materials and Methods. A one-compartment model following fractal Michaelis-Menten kinetics under a steady state is developed and applied to concentration-time data for the cardiac drug mibefradil in dogs. The model predicts a fractal reaction order and a power law asymptotic time-dependence of the drug concentration, therefore a mathematical relationship between the fractal reaction order and the power law exponent is derived. The goodness-of-fit of the model is assessed and compared to that of four other models suggested in the literature.
Results. The proposed model provided the best fit to the data. In addition, it correctly predicted the power law shape of the tail of the concentration-time curve.
Conclusion. A simple one-compartment model with steady state fractal Michaelis–Menten kinetics describing drug elimination from the body most accurately describes the pharmacokinetics of mibefradil in dogs. The new fractal reaction order can be explained in terms of the complex geometry of the liver, the organ responsible for eliminating the drug.

KEY WORDS: drug elimination; fractals; Michaelis-Menten kinetics; pharmacokinetics; power laws.

INTRODUCTION

Pharmacokinetics is the study of the absorption, distribution, metabolism, and eventual elimination of a drug from the body (1). Pharmacological data usually consist of discrete values of the concentration of a drug in the plasma or blood as a function of time. A plot of these values generates a concentration-time curve that first rises as absorption of the drug dominates and then decreases after a maximum concentration value is reached. This decline may be relatively short or may last for several days, and it is mainly governed by the rate of elimination of the drug from the body. The goal of pharmacokinetic modeling is to use these curves to describe, compare, and predict a drug's course in the body, as well as to determine optimum dosing regimes, potential toxicity, and drug–drug interactions.

Classical compartmental models are the most common type of pharmacokinetic models. However, while they can provide adequate agreement with clinical pharmacokinetic data sets, they often fail to provide a good fit to the tail regions, where non-exponential time-dependence can occur that is better fit by power laws or gamma functions (2,3). Since all data sets are finite in size, they can always be fit with a sufficiently large number of compartments and an associated large number of adjustable parameters. However, this does not address the origin of the non-exponential behaviour in pharmacokinetics. A link has been made previously (4) to the connection between concentration-time curves with power law tails and fractal kinetics. The objectives of this paper are to i) identify the existence of long-time tails in the concentration-time curves of mibefradil in dogs, ii) apply the theory of fractal enzyme kinetics under steady state conditions to a pharmacokinetic model, and iii) demonstrate how the model both provides an improved fit to the data and predicts the existence of the power law tails.

THEORY

Compartmental models are the most common type of pharmacokinetic models (5). A compartment is defined as the number of drug molecules having the same probability of undergoing a set of chemical kinetic processes. The exchange of drug molecules between compartments is described by kinetic rate coefficients. The classical compartmental model is based on two main assumptions: i) each compartment is homogenous (i.e., there is instantaneous mixing), and ii) the kinetic rate coefficients are all constant, such that the fraction of drug transferred between any two compartments is constant in time. The system is described by coupled first-order differential equations whose solutions take the form of a sum of terms that are exponential in time.

Classical kinetics is based on the law of mass action, which states that the rate v of a chemical reaction is directly

[1] P-412, Avadh Bhatia Physics Laboratory, Department of Physics, Faculty of Science, University of Alberta, Edmonton, AB T6G 2J1, Canada.
[2] To whom correspondence should be addressed. (e-mail: rmarsh@ualberta.ca)

proportional to the product of the concentrations of the N reactants each raised to the order n_i:

$$v = k\prod_{i=1}^{N} C_i^{n_i}, \tag{1}$$

where C_i is the concentration of reactant i and k is the kinetic rate coefficient in units of time^{-1}. The reaction order n_i is the number of concentration terms that must be multiplied together to get the rate of the reaction (6). For a single step, n_i is typically equal to the molecularity, which is the number of molecules that are altered during the reaction. When only one molecule is modified, the reaction is given by

$$v = kC. \tag{2}$$

Enzyme Kinetics and the Michaelis-Menten Equation

The rate of enzyme-catalyzed reactions can deviate from those predicted by classical kinetics. Michaelis-Menten kinetics (7) is the standard formalism for describing these reactions. At high concentrations, saturation of the enzymes limits the maximum reaction rate that can be achieved, while at low concentrations, the rate of formation of the enzyme-substrate complex becomes significant and the reaction becomes dependent on the substrate concentration (8).

Consider the reaction:

$$E + S \underset{k_{-1}}{\overset{k_1}{\rightleftharpoons}} ES \xrightarrow{k_2} E + P \tag{3}$$

where E, S, ES, and P represent the enzyme, substrate, enzyme-substrate complex, and product, respectively. If we denote the concentration of the substrate as C, the concentration of the substrate-enzyme complex as x, and the total concentration of enzyme as e_0, the system is described by the following ordinary differential equations:

$$\frac{dx}{dt} = k_1(e_0 - x)C - (k_{-1} + k_2)x, \tag{4}$$

$$\frac{dp}{dt} = k_2 x. \tag{5}$$

Using the Briggs-Haldane treatment (6) to simplify the problem, a quasi-steady-state assumption is made where the concentration of the substrate-enzyme complex is taken to be constant, i.e., $dx/dt = 0$, and the Michaelis-Menten equation is:

$$v = \frac{v_{\max} C}{k_M + C}. \tag{6}$$

The parameter $v_{\max}$ is the maximum velocity of the reaction, and the Michaelis-Menten constant K_M is the substrate concentration at half the maximum velocity.

Asymptotics of the Concentration-Time Curve

The solution to a compartmental model with constant coefficients takes the form of a linear superposition of exponential terms, and the resulting concentration-time curve exhibits an exponentially decaying tail. However, there is evidence that the concentration-time curves of many drugs exhibit long-time power law tails of the form

$$C(t) \sim t^{-\gamma} \quad \text{for } t > T, \tag{7}$$

where T marks the time of the onset of the tail. Negative power laws were first applied, empirically, to describe the washout of bone-seeking radioisotopes (9,10). Subsequently, other types of clearance curves have been fit by a single power law, two sequential power laws, or the gamma function $y(t) = at^{-\alpha}e^{-\beta t}$ (2,3,11,12). Different explanations for these fits have been proposed, including a stochastic random walk model based on the cycling of molecules in and out of the plasma (13), a set of convection–diffusion equations for transit in the liver (3), and gamma-distributed drug residence times (14).

In this paper, we introduce a model based on fractal kinetics with an anomalous reaction order as a physiologically-based mechanism that generates power law tails using only one compartment. This model is naturally interpreted in terms of the anatomy and physiology of the liver, which is the organ predominantly responsible for drug elimination.

Transient Fractal Kinetics

Anacker and Kopelman (15) found that reactions that occur on or within fractal media exhibit anomalous kinetics that do not follow the classical mass-action form. Specifically, the kinetic rate coefficient is time-dependent (16):

$$k = k_0 t^{-h}, \tag{8}$$

where

$$h = 1 - \frac{d_s}{2}. \tag{9}$$

The quantity d_s is the spectral dimension that describes the path of a random walker within the medium (17). The classical case corresponds to $d_s = 2$. Equations (8) and (9) have been supported by experiments of trapping and binary reactions on the Sierpinski gasket, percolation clusters, and lattices with disordered transition rates (16,18–20). While Eq. (8) applies to diffusion-limited reactions on fractals, it also applies to any situation for which $h > 0$.

Equation (8) has been incorporated into pharmacokinetics through both non-compartmental and compartmental models. The former includes the homogeneous–heterogeneous distribution model introduced by Macheras (21) to quantify the global and regional characteristics of blood flow to organs. The latter includes the fractal compartmental model developed by Fuite *et al.* (22) in which a classical compartment was used to represent the plasma while a fractal compartment was used to represent the liver. In this formalism, the rate of elimination from the liver is given by

$$v = k_0 t^{-h} C. \tag{10}$$

Simulations of the model showed that h plays a significant role in determining the shape of the concentration-time curve (4).

Several attempts have been made to incorporate Eq. (8) into the Michaelis-Menten equation to describe concentration-dependent reactions that occur in spatially constrained conditions. Kosmidis *et al.* (23) made the substitution $k_1 = k_1^0 t^{-h}$ into Eq. (4), producing the formula

$$v = \frac{v_{\max} C}{K_{M0} t^h + C}. \tag{11}$$

They also performed Monte Carlo simulations and found that Eq. (11) holds mainly when the initial substrate concentration is high, either through an intravenous (IV) bolus administration or a high rate of absorption. In addition, they incorporated Eq. (11) into a one-compartment model. Berry (24) used Monte Carlo simulations on a 2D lattice to model enzyme reactions in low-dimensional media, and he found that h increases independently with increasing obstacle density on the lattice and increasing initial substrate concentration. Simulations performed by Aranda *et al.* (25) also confirm these results but suggest that K_{M0} is characterized by multifractality and hence a set of fractal exponents.

Steady State Fractal Kinetics

As seen above, the effect of complex geometry on the rate of transient reactions produces an anomalous kinetic rate coefficient. Anacker and Kopelman (15) demonstrated that under steady state conditions, however, the effect of the geometry is manifested as an anomalous reaction order. They showed that Eq. (2) should be replaced by the effective rate equation

$$v = kC^X, \tag{12}$$

where X is a fractal reaction order related to the spectral dimension of the random walk. For example (26),

$$X = \begin{cases} 1 + \frac{2}{d_s} \text{ for } A + A \text{ reactions,} \\ 1 + \frac{4}{d_s} \text{ for } A + B \text{ reactions.} \end{cases} \tag{13}$$

These equations have been confirmed using Monte Carlo simulations. Anacker *et al.* (18) found that $X = 2.44$ for the 2D Sierpinski gasket and $X = 2.01$ as expected for the homogenous cubic lattice. Klymko and Kopleman (27) found that for bimolecular reactions in solids, X ranged from the homogeneous value of 2 up to a value of 30. Newhouse and Kopelman (28) found values of $X \approx 5$ for ensembles of 10×10 islands and $X \approx 15$ for ensembles of 5×5 islands. Therefore, as a space becomes more finely divided, as in the example a fractal dust like the Cantor set (29), $d_s \to 0$ and $X \to \infty$.

A form of concentration-dependent fractal kinetics was developed by López-Quintela and Casado (30), who proposed the following scaling relationship:

$$k^{eff} = AC^{1-d_f} \quad 0 \le d_f \le 1, \tag{14}$$

where d_f is the fractal dimension of the space. The effective kinetic rate coefficient k^{eff} is therefore assumed to be dependent on the observation scale, here taken to be the concentration. By applying this equation to $v_{\max}$, they obtained the formula:

$$v = \frac{v_{\max}^{eff} C^{2-d_f}}{K_M^{eff} + C}, \tag{15}$$

where $v_{\max}^{eff}$ and K_M^{eff} are new constants. For $d_f = 1$, the classical Michaelis–Menten equation is recovered, and as $d_f \to 0$, the complexity of the reaction becomes more and more important. Heidel and Maloney (31) performed an analytical exploration of this equation, and initially Macheras (32) and later Ogihara (33) applied it to model carrier-mediated transport under heterogeneous conditions.

A seemingly different approach to concentration-dependent fractal kinetics is the "power-law formalism" developed by Savageau (34), expressed through the generalized mass-action representation:

$$\frac{dC_i}{dt} = \sum_{k=1}^{r} \alpha_{ik} \prod_{j=1}^{n} C_j^{g_{ijk}} - \sum_{k=1}^{r} \beta_{ik} \prod_{j=1}^{n} C_j^{h_{ijk}}, \tag{16}$$

where α and β are the kinetic rate coefficients and g and h are the kinetic rate orders associated with each reactant. The equations for the power-law formalism are complicated and Savageau admits that this model works best for large series of reactions rather than one or more reactions catalyzed by only one enzyme (34). Savageau justifies his formalism by showing that for homodimeric reactions, its equations are equivalent to the fractal kinetics equations. However, this equivalence has yet to be proven for any other reactions due to the complexity of the equations (35). In principle, it is possible that Eq. (16) can be obtained by summing over several Michaelis-Menten reactions.

To summarize, any reaction for which $h > 0$ or $X > n$ is referred to as following fractal-like kinetics (36). In this paper, an alternative formulation of dose-dependent fractal kinetics is proposed based on fractal reaction orders under steady state conditions.

MATERIALS AND METHODS

Model

In a strict sense, a steady state regime means that the concentration of the reactant is constant in time, i.e., $dC/dt = 0$. One way in which this can be achieved is if the concentration of drug molecules is much greater than the concentration of enzymes, even if the local concentration values vary considerably. Even in the presence of drug elimination, a steady state can be maintained due to the recycling of drug molecules by the circulatory system. It is important to distinguish this steady state achieved through recycling from the steady state defined for chronic drug administration. In the latter, drug is administered through multiple doses or a constant infusion, and the elimination rate eventually becomes equal to the infusion rate. The steady state in the current theory can be considered as a local approximation to the same condition.

If the environment is heterogeneous, the system is described by the equations:

$$\frac{dx}{dt} = k_1(e_0 - x)C^X - (k_{-1} + k_2)x, \tag{17}$$

$$\frac{dp}{dt} = k_2 x. \tag{18}$$

Applying the quasi-steady-state assumption, $dx/dt = 0$, the following equation is derived:

$$v = \frac{v_{\max} C^X}{K_M + C^X} \tag{19}$$

It can be noted that Eq. (19) has the same form as the Hill equation that describes the response of a patient or tissue as a function of the drug concentration (8). Incorporating this formula into a one-compartment model with an IV infusion yields

$$\frac{dC}{dt} = -\frac{v_{\max} C^X}{K_M + C^X} + \frac{i(t)}{V_d}, \tag{20}$$

where $i(t)$ is the infusion rate in units of mass/time and V_d is the volume of distribution in units of volume.

To investigate the asymptotics of Eq. (20), we consider the model post-infusion. For high concentrations (those occurring well above K_M):

$$\frac{dC}{dt} = -v_{\max}. \tag{21}$$

For low concentrations (those occurring far below K_M):

$$\frac{dC}{dt} = -\frac{v_{\max}}{K_M} C^X. \tag{22}$$

Integrating Eq. (22) leads to the asymptotic power law behaviour

$$C(t) \sim t^{\frac{1}{1-X}}. \tag{23}$$

Comparing to Eq. (7) yields the relationship

$$\gamma = \frac{1}{1 - X} \tag{24}$$

or

$$X = 1 - \frac{1}{\gamma}. \tag{25}$$

Note that Eqs. (23–25) are undefined for $X = 1$, since this value corresponds to the classical model with an exponential tail, which is inconsistent with a power law.

The fact that the proposed steady state model predicts long-time power law behaviour provides a point of comparison with other models. The Michaelis-Menten model predicts an exponential tail, and the transient fractal and fractal Michaelis-Menten equations predict stretched exponential tails of the form $\sim\exp(at^{1-h})$.

Data Analysis

Concentration-time data were obtained for the cardiac drug mibefradil (37) in four dogs. The dogs received a dose of 1 mg/kg of mibefradil infused over 10 min. The analysis of the data consists of the following steps: (1) quantification of the shape of the tail, (2) comparison of the fit of the proposed model with that of existing models, and (3) testing of the relationship expressed in Eq. (25).

The value and standard deviation of the power law tail exponent γ were calculated from the concentration-time curves using linear regression analysis of the log-transformed data.

The models were fit to the data using a parameter optimization method based on a simulated annealing (SA) algorithm implemented in C++. The SA algorithm (38) minimizes an objective function through an efficient exploration of the parameter space. All downhill moves are accepted and selective uphill moves are allowed according to the Metropolis algorithm and an effective temperature. At the start of the annealing process, the temperature is relatively high compared to the standard deviation of the objective function, and the probability of accepting an uphill move is great. Hence, the random walk is able to explore a wide area of parameter space without getting trapped in local minima. As the temperature is decreased, the algorithm is able to focus in on the most promising areas and locate the global minimum.

The SA algorithm has many advantages over other optimization methods. It is largely independent of the starting values, it can escape local minima through selective uphill moves, and the underlying function need not be continuous. The SA method has been found to be superior to the simplex method, the Adaptive Random Search, the quasi-Newton algorithm, and the Levenberg-Marquardt algorithm in finding the optimum of continuous functions (39–41).

The objective function was chosen to be the weighted residual sum of squares (WRSS) (42):

$$\mathrm{WRSS} = \sum_{i=1}^{n} \left[\frac{\left(C_i - \widehat{C}_i\right)^2}{\widehat{C}_i^2} \right], \tag{26}$$

where $\widehat{C}_i$ denotes the predicted value of C_i based on the given model. The goodness-of-fit of each model was assessed using the Akaike Information Criterion (AIC), which takes

Table I. Summary of Models for the Enzyme-Mediated Kinetics of Drug Elimination

Model	Reference	Abbreviation	Reaction Rate
Fractal	(22)	F	$k_0 t^{-h} C$
Michaelis-Menten	(7)	MM	$\frac{v_{\max} C}{K_M + C}$
Transient fractal Michaelis-Menten	(23)	FMM	$\frac{v_{\max} C}{K_{M0} t^h + C}$
López–Quintela fractal Michaelis-Menten	(30)	LQC	$\frac{v_{\max}^{eff} C^{2-d_f}}{K_M^{eff} + C}$
Steady state fractal Michaelis-Menten		SSFMM	$\frac{v_{\max} C^X}{K_M + C^X}$

Table II. Slope γ of the Log(Concentration) *versus* Log(Time) Curve Between t = 30 min and t = 1440 min

Dog	γ	R^2
1	−0.702 (0.028)	0.991
2	−0.464 (0.049)	0.927
3	−0.597 (0.024)	0.989
4	−0.705 (0.066)	0.943

Values are given as mean (standard deviation).

into account the WRSS as well as the number of model parameters, N_{par}, and the number of data points, N_{obs} (42):

$$\text{AIC} = N_{\text{obs}} \ln(\text{WRSS}) + 2N_{\text{par}}. \quad (27)$$

A lower value indicates a better fit. Five one-compartment models were fit to the data sets, and they are summarized in Table I.

RESULTS

The shape of the tail was determined for the four data sets and was found to be a straight line on a log–log plot, indicating a power law relationship. The values for the power law exponent γ are listed in Table II. The power law tail extends over three orders of magnitude in time, and the goodness-of-fit represented by the R^2 value is greater than 0.9 for every dog. This result indicates that the SSFMM model is an appropriate model for the data.

The results from the model fits are listed in Table III. The MM model performs the worst. Furthermore, the values that it predicts for the volume of distribution are unrealistically low for three of the four dogs. In contrast, the V_d values for the other models are reasonable for a dog and are consistent with each other. Furthermore, the K_M values for the MM model are almost two orders of magnitude higher than the values for the LQC, FMM, and SSFMM models. The values for the intrinsic clearance, $v_{\max}/K_M$, are also at least one order of magnitude smaller than those predicted by the other models. These results indicate that classical Michaelis-Menten kinetics does not adequately describe the elimination of mibefradil from the dog.

The LQC, F, and FMM models provide some improvement. However, in the case of the LQC model, the reaction orders of $2-d_f$ yield values of zero for the fractal dimension, d_f, essentially eliminating the fractal nature of the model. In the case of the F and FMM models, the exponent h takes the maximum value of 1.

Table III. One-Compartment Parameters for the Drug Concentration in the Jugular Vein of Dogs Following a 10-min Infusion of 1 mg/kg of Mibefradil

		Value				
Model	Parameter	Dog 1	Dog 2	Dog 3	Dog 4	Mean
MM	$v_{\max}$(ng/ml/min)	327	4,699	4,737	4,375	
	K_M(ng/ml)	96,593	101,139	100,131	101,046	
	V_d(l)	10.5	0.00369	0.00361	0.00405	
	WRSS	7.27	11.0	11.0	11.0	
	AIC	31.8	37.2	37.2	37.2	35.9
LQC	$v_{\max}^{eff}$ (ng/ml/min)	587	847	363	623	
	K_M^{eff} (ng/ml)	5,323	6,961	4,702	5,693	
	V_d(l)	7.21	8.45	4.64	5.67	
	2-D	2.00	2.00	2.00	2.00	
	WRSS	2.68	4.06	4.15	3.05	
	AIC	20.8	26.2	26.5	22.5	24.0
F	k_0(/min)	1.01	1.16	1.03	1.21	
	V_d(l)	4.80	4.31	4.95	3.55	
	h	0.999	0.999	0.998	0.998	
	WRSS	2.56	5.33	3.74	4.14	
	AIC	18.2	27.8	23.2	24.5	23.4
FMM	$v_{\max}$(ng/ml/min)	4,358	3,306	2,486	4,170	
	K_{M0} (ng/ml)	4,623	3,638	2,709	4,401	
	V_d(l)	6.04	11.0	10.1	12.0	
	h	1.00	1.00	1.00	1.00	
	WRSS	2.01	1.82	2.01	2.01	
	AIC	17.1	15.8	17.1	17.1	16.8
SSFMM	$v_{\max}$(ng/ml/min)	3,575	8,201	3,548	3,817	
	K_M (ng/ml)	5,217	799	6,778	7,098	
	V_d(l)	1.30	2.39	16.5	9.54	
	X	2.56	3.35	2.74	2.61	
	WRSS	0.845	0.263	0.219	0.544	
	AIC	5.99	−9.38	−11.7	0.0797	−3.75

Table IV. Comparison Between the Values for the Fractal Reaction Order X Predicted from the Slope γ and Obtained from the Model Fit

	X	
Dog	Predicted from γ	Model value
1	2.42 (0.10)	2.56
2	3.16 (0.33)	3.35
3	2.68 (0.11)	2.74
4	2.41 (0.22)	2.61

The SSFMM model provides the best fit to all data sets. The values for X determined from the model fit were compared to those calculated from the power law tail exponent γ using Eqs. (23) and (25), and the results are listed in Table IV. The values agree within error for all but Dog 1. Fig. 1a) shows the power law tail for Dog 3, and Fig. 1b) shows the same data fit by the SSFMM model. The proposed model accurately describes the concentration-time curve at all concentration levels.

According to Eq. (22), the existence and onset of the power law tail correlate with the value of K_M, and the power law behaviour should only exist for $C << K_M$. The values

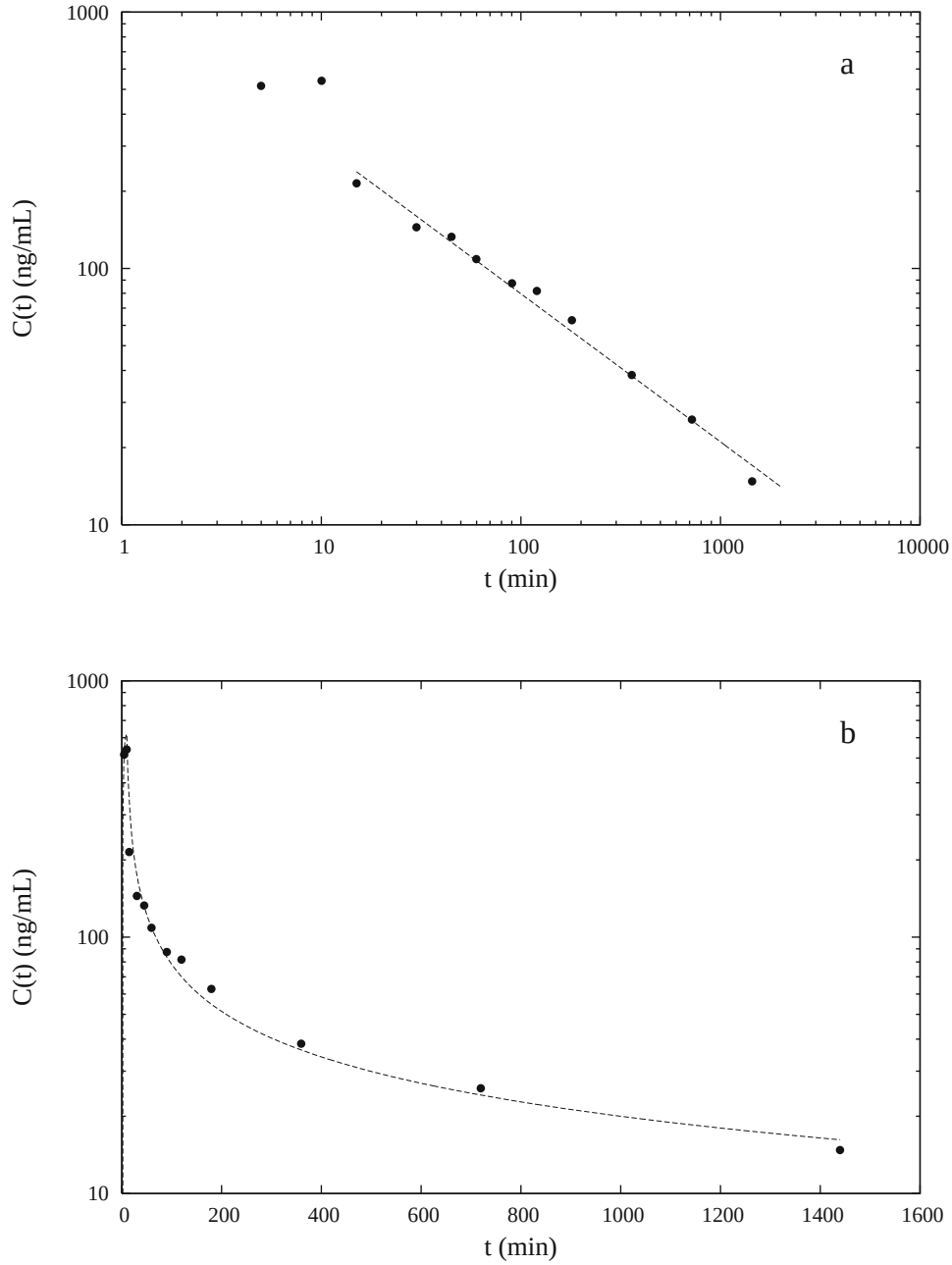

Fig. 1. Concentration-time curves for mibefradil data for Dog 3. (a) Log–log plot showing the long-time power law tail from 30 to 1,440 min. The dashed line is the regression line with $\gamma = -0.597 \pm 0.024$. (b) The same data but the dashed line now represents the best-fit curve found using the steady state fractal model with $X = 2.74$.

estimated for K_M by the SSFMM model range from 800 ng/ml to 7,000 ng/ml and are between 30 and 90% higher than the maximum plasma concentrations (556.1 to 1,400 ng/ml). Therefore, the power law tails are observable because the dose of mibefradil given to the dogs in this study leads to plasma concentrations well below saturation levels. Furthermore, Eq. (22) can be interpreted alternatively in terms of a concentration-dependent $v_{\max}$ of the form $v_{\max}^{eff} = v_{\max} C^{X-1}$. When the approximate Eq. (22) was used instead of Eq. (19), it resulted in similar parameter values as the SSFMM model but with a poorer fit to the rise of the curve.

DISCUSSION

One-compartment models are simplifications; however, they can provide an accurate and adequate fit if the distribution of the drug is rapid and equilibrium is achieved quickly in all tissues. In this study, we used a one-compartment model to show that anomalous reaction orders can be a reflection of the heterogeneous nature of the medium under which drug metabolism occurs. Two concepts need to be elaborated upon: the meaning of a steady state and the meaning of noninteger reaction orders.

It is well-known that the liver has a complex geometry. The blood vessels supplying it are arranged as a fractal tree (43), its cellular network has fractal properties (44), and the perfusion of blood at the terminal branches is heterogeneous (45). Both transient and steady state reactions occurring within such spaces can exhibit anomalous behaviour. For transient reactions, it is assumed that there is a random distribution of reactants (36). Therefore, anomalous kinetics in the transient case strictly results from the decreased efficiency of random walkers in exploring their irregular space (quantified by d_s). In the steady state regime, however, there is an influx of molecules. In regular geometries, this influx can cause a net stirring effect (36); however, in fractal and confined geometries, self-stirring is inefficient. The spaces are instead characterized by large fluctuations in the local concentration and an increasing segregation of molecules (26). This effect has been reported for reaction–diffusion phenomena in physical systems (46). As a result, under steady state conditions, the distribution of molecules is partially ordered due to the influx of molecules, and the nonrandomness reduces the reaction probabilities and consequently the reaction rate. To summarize, transient fractal kinetics occur in well-stirred heterogeneous media while steady state kinetics occur in poorly stirred heterogeneous media. Here, the term heterogeneous describes to the geometry of the environment.

In the case of steady state fractal kinetics, Klymko and Kopelman (27) interpreted noninteger values of X as characteristic of a microscopically heterogeneous medium that is best described as a collection of kinetically independent clusters. The kinetic rate coefficients are then kinetic averages taken over domains of different sizes and local concentration. This interpretation is consistent with the studies that reported high X values for reactions occurring on clusters and islands (28,47). A similar model can be developed for the liver, the organ predominantly responsible for the elimination of mibefradil from the body. The metabolic enzymes are located in the liver cells, called hepatocytes, which are organized around the terminal supply vessels. Each set of vessels and their surrounding cells are called a sinusoid. Not only does each sinusoid have a different number and distribution of hepatocytes, it receives a different portion of the blood flow. Therefore, the liver can be considered as a network of clusters of sinusoids. Because X increases as the size of the clusters decreases (28), $X = 1$ means that the liver acts as a homogeneous, well-mixed compartment and $X > 1$ indicates segmentation and a lack of mixing.

This interpretation is consistent with a model proposed by Weiss (45), who described the transit times in the liver as being determined by both the micromixing and macromixing processes. He suggested two models at different ends of the spectrum: i) a distributed model in which the sinusoids are parallel and there is complete segregation of the pathways, and ii) a dispersion model in which the sinusoids are interconnected and there is perfect micromixing. Considering our results in this framework, X provides a quantitative measure of the degree of micromixing between sections of the liver and locates the model somewhere between Weiss's two extreme models.

CONCLUSION

This paper provides the first application of fractal kinetics under steady state conditions to pharmacokinetics. We have demonstrated that a steady state fractal Michaelis-Menten equation best describes the elimination of the drug mibefradil from dogs. Furthermore, it accounts for the long-time power law behaviour of the concentration through the inclusion of a fractal reaction order, X. This anomalous reaction order suggests that the liver, the organ of elimination for mibefradil, is best treated as a collection of clusters of sinusoids. The higher the value of X, the less mixing that occurs between adjacent sinusoid clusters.

We conclude that transient fractal kinetics is appropriate for describing reactions that occur within well-mixed heterogeneous environments, while steady state fractal kinetics better describes reactions that occur in understirred heterogeneous spaces. The latter can occur due to the continuous influx of drug molecules through recycling in the circulatory system. Finally, although the proposed one-compartment model is sufficient for fitting curves with a single power law tail, curves described by consecutive power laws may require more than one compartment.

ACKNOWLEDGMENTS

The authors would like to thank Dr. Y. K. Tam for providing the mibefradil data sets as well as Mathematics of Information Technology and Complex Systems (MITACS) for funding during the preparation of this manuscript. J.A.T. would also like to thank the Allard Foundation.

REFERENCES

1. M. Gibaldi and D. Perrier. *Pharmacokinetics*, Marcel Dekker, New York, (1982).
2. M. E. Wise. The evidence against compartments. *Biometrics* **27**:262 (1971).
3. K. H. Norwich and S. Siu. Power functions in physiology and pharmacology. *J. Theor. Biol.* **95**:387–398 (1982).

4. P. Chelminiak, R. E. Marsh, J. A. Tuszyski, J. M. Dixon, and K. J. E. Vos. Asymptotic time dependence in the fractal pharmacokinetics of a two-compartment model. *Phys. Rev. E.* **72**:031903 (2005).
5. J. A. Jacquez. *Compartmental Analysis in Biology and Medicine*, BioMedware, Ann Arbor (1996).
6. A. Cornish-Bowden. *Fundamentals of Enzyme Kinetics*. Portland, London, (1995).
7. L. Michaelis and M. L. Menten. Die kinetik der invertinwirkung. *Biochem. Z.* **49**:333–369 (1913).
8. J. D. Murray. *Mathematical Biology*. Springer, Berlin Heidelberg New York, (1989).
9. W. P. Norris, S. A. Tyler, and A. M. Brues. Retention of radioactive bone-seekers. *Science* **128**:456–462 (1958).
10. M. E. Wise. Interpreting both short- and long-term power laws in physiological clearance curves. *Math. Biosci.* **20**:327–337 (1974).
11. J. Anderson, S. B. Osborn, R. W. Tomlinson, and M. A. Weinbren. Some applications of power law analysis to radioisotope studies in man. *Phys. Med. Biol.* **8**:287–295 (1963).
12. J. B. Bassingthwaighte and D. A. Beard. Fractal 15O-labeled water washout from the heart. *Circ. Res.* **77**:1212–1221 (1995).
13. M. E. Wise, S. B. Osborn, J. Anderson, and R. W. S. Tomlinson. A stochastic model for turnover of radiocalcium based on the observed power laws. *Math. Biosci.* **2**:199–224 (1968).
14. M. Weiss. Use of gamma distributed residence times in pharmacokinetics. *Eur. J. Clin. Pharmacol.* **25**:695–702 (1983).
15. L. W. Anacker and R. Kopelman. Fractal chemical kinetics: simulations and experiments. *J. Chem. Phys.* **81**:6402–6403 (1984).
16. R. Kopelman. Rate processes on fractals: theory, simulations, and experiments. *J. Stat. Phys.* **42**:185–200 (1986).
17. S. Alexander and R. Orbach. Density of states on fractals: "fractons". *J. Phys. Lett.* **43**:L-625–L-631 (1982).
18. L. W. Anacker, R. Kopelman, and J. S. Newhouse. Fractal chemical kinetics: reacting random walkers. *J. Stat. Phys.* **36**:591–602 (1984).
19. S. Havlin, R. Kopelman, R. Schoonover, and G. H. Weiss. Diffusive motion in a fractal medium in the presence of a trap. *Phys. Rev. A.* **43**:5228–5232 (1991).
20. P. W. Klymko and K. Kopelman. Fractal reaction kinetics: exciton fusion clusters. *J. Phys. Chem.* **87**:4565–4567 (1983).
21. P. Macheras. A fractal approach to heterogeneous drug distribution: calcium pharmacokinetics. *Pharm. Res.* **13**:663–670 (1996).
22. J. Fuite, R. E. Marsh, and J. A. Tuszynski. Fractal pharmacokinetics of the drug mibefradil in the liver. *Phys. Rev. E* **66**:021904 (2002).
23. K. Kosmidis, V. Karalis, P. Argyrakis, and P. Macheras. Michaelis–Menten kinetics under spatially constrained conditions: application to mibefradil pharmacokinetics. *Biophys. J.* **87**:1498–1506 (2004).
24. H. Berry. Monte Carlo simulations of enzyme reactions in two dimensions: fractal kinetics and spatial segregation. *Biophys. J.* **83**:1891–1901 (2002).
25. J. S. Aranda, E. Salgado, and A. Muñoz-Diosdado. Multifractality in intracellular enxymatic reactions. *J. Theor. Biol.* **240**: 209–217 (2006).
26. L. W. Anacker and R. Kopelman. Steady-state chemical kinetics on fractals: segregation of reactants. *Phys. Rev. Lett.* **58**:289–291 (1987).
27. P. W. Klymko and K. Kopelman. Heterogeneous exciton kinetics: triplet naphthalene homofusion in an isotropic mixed crystal. *J. Phys. Chem.* **86**:3686–3688 (1982).
28. J. S. Newhouse and R. Kopelman. Reaction kinetics on clusters and islands. *J. Chem. Phys.* **85**:6804–6806 (1986).
29. B. B. Mandelbrot. *The Fractal Geometry of Nature*, Freeman, San Francisco, (1982).
30. M. López-Quintela and J. Casado. Revision of the methodology in enzyme kinetics: a fractal approach. *J. Theor. Biol.* **139**:129–139 (1989).
31. J. Heidel and J. Maloney. An analysis of a fractal Michaelis-Menten curve. *J. Aust. Math. Soc. Series B, Appl. Math* **41**:410–422 (2000).
32. P. Macheras. Carrier-mediated transport can obey fractal kinetics. *Pharm. Res.* **12**:541–548 (1995).
33. T. Ogihara, I. Tamai, and A. Tsuji. Application of fractal kinetics for carrier-mediated transport of drugs across intestinal epithelial membrane. *Pharm. Res.* **15**:620–625 (1998).
34. M. A. Savageau. Development of fractal kinetic theory for enzyme-catalysed reactions and implications for the design of biochemical pathways. *Biosystems* **47**:9–36 (1998).
35. S. Schnell and T. E. Turner. Reaction kinetics in intracellular environments with macromolecular crowding: simulations and rate laws. *Prog. Biophys. Mol. Biol.* **85**:235–260 (2004).
36. R. Kopelman. Fractal reaction kinetics. *Science* **241**:1620–1626 (1988).
37. A. Skerjanec, S. Tawfik, and Y. K. Tam. Nonlinear pharmacokinetics of mibefradil in the dog. *J. Pharm. Sci.* **85**:189–192 (1996).
38. S. Kirkpatrick, C. Gelatt, and M. Vecchi. Optimization by simulated annealing. *Science* **220**:498–516 (1983).
39. A. Corana, M. Marchesi, C. Martini, and S. Ridella. Minimizing multimodal functions of continuous variables with the "simulated annealing" algorithm. *ACM Trans. Math. Softw.* **13**:262–280 (1987).
40. W. L. Goffe, G. D. Ferrier, and J. Rogers. Global optimization of statistical functions with simulated annealing. *J. Econom.* **60**:65–99 (1994).
41. A. Eftaxias, J. Font, A. Fortuny, A. Fabregat, and F. Stüber. Nonlinear kinetic parameter estimation using simulated annealing. *Comput. Chem. Eng.* **26**:1725–1733 (2002).
42. J. Gabrielsson and D. Weiner. *Pharmacokinetic/Pharmacodynamic Data Analysis: Concepts and Applications*, Swedish Pharmaceutical, Stockholm, (1997).
43. C. Javanaud. The application of a fractal model to the scattering of ultrasound in biological media. *J. Acoust. Soc. Am.* **86**:493–496 (1989).
44. E. Gaudio, S. Chaberek, A. Montella, L. Pannarale, S. Morini, G. Novelli, F. Borghese, D. Conte, and K. Ostrowski. Fractal and Fourier analysis of the hepatic sinusoidal network in normal and cirrhotic rat liver. *J. Anat.* **207**:107–115 (2005).
45. M. Weiss. A note on the interpretation of tracer dispersion in the liver. *J. Theor. Biol.* **184**:1–6 (1997).
46. S. Cornell, M. Droz, and B. Chopard. Role of fluctuations for inhomogeneous reaction–diffusion phenomena. *Phys. Rev. A* **44**:4826–4832 (1991).
47. J. S. Newhouse and R. Kopelman. Steady-state chemical kinetics on surface clusters and islands: segregation of reactants. *J. Phys. Chem.* **92**:1538–1541 (1988).